Proceedings of the Symposium on Fundamental Gas-Phase and
Surface Chemistry of Vapor-Phase Materials Synthesis,
PV98-28, p. 153,The Electrochemical Society, 1998.

IN SITU STUDIES OF TEOS/OZONE CVD: EXPERIMENTAL CONSIDERATIONS FOR PROBING REACTIONS IN COMMERCIAL CVD EQUIPMENT

Thomas K. Whidden[a], Sun Young Lee[a], Xiaoyi Bao[b], Michel Couturier[c], James Taylor[d], Ping Lu [b], Sebastien Romet[c] and Zhao Xiaozhong[d]

[a]Xylaur enterprises, Fredericton, New Brunswick, Canada E3B 6C2;
[b] Physics Department, [c] Chemical Engineering Department, [d] Electrical Engineering Department, University of New Brunswick, Fredericton, New Brunswick, Canada E3B 6C2;

In situ FT-IR of TEOS/ozone CVD reactions in production-style systems is described. The method shows excellent sensitivity to reaction precursors and products. It is shown that conventional spectrometer configurations have to be modified to effectively sample that region of the reactor space in which the reactive chemistry occurs. Modeling studies are described that show this layer to have a thickness of ca. 2-mm. Fiber optic approaches are described that will partially fulfill the beam requirements for CVD reactor analyses.

INTRODUCTION

TEOS/ozone chemistries fulfill the low thermal budget requirements of ULSI processing, retain many of the desirable properties of other TEOS-based processes, and exhibit self-planarizing characteristics superior to any other oxide deposition process (1-3). Two unresolved issues exist for TEOS/ozone processes. First, the as-deposited films are hygroscopic, retaining residual silanols (Si-OH) and water. Annealing, the normal route to remove silanols and water from oxide thin films is not viable for TEOS/ozone applications as it negates the advantages of low temperature processing. Second, TEOS/ozone processes operating near the temperature limits to minimize water and silanol concentrations exhibit narrow windows for low-particulate processing. Process-derived particles are due to parasitic side reactions (4) that are enhanced at elevated temperature. Successful production processes thus require a fine balance of conditions to accommodate diametrically opposed thermal processing requirements in order to achieve acceptable film quality vs. low process particle accumulations. *In situ* monitoring of the TEOS/ozone process can greatly assist in maintaining this balance.

Characterizational work on the TEOS/ozone process is available in the literature. Mass spectral, gas chromatographic and other evidence (5-9) supports the participation of transient gas phase intermediates in TEOS/ozone chemistries. The literature suggests a mechanism for both film formation and particle growth that includes a step-wise polymerization initiated by the reaction of TEOS and atomic oxygen. Particle nucleation and growth is then due to the further condensation of hydroxylated polysiloxanes within this mechanistic context. Inferential data based on film growth characteristics support this mechanism and the presence and active participation of at least two siloxane intermediate species (10). Oligomeric siloxanes and hydroxy-siloxanes have been

observed in GC-MS studies of TEOS/ozone APCVD depositions, albeit using off-line sampling techniques (9).

This work describes analyses of TEOS/ozone reactions within a CVD chamber using FT-IR spectroscopy. We discuss the use of chemical kinetic modeling for insight into the most appropriate sampling configurations for *in situ* analyses. We describe the results of our *in situ* measurements of process gasses in the chamber and discuss these results within a context of literature data and correlations of the spectra with the chemical properties of the films produced in the process. Finally, we describe the consequences of our modeling and experimental studies for spectroscopic configurations to be used in monitoring production CVD systems.

EXPERIMENTAL

We modeled the TEOS/ozone CVD process using CHEMKIN-III (11,12). CVD reactions were performed in a system of our own design (13,14). Spectra were obtained using a customized Bomem MB series FT-IR with a liquid-nitrogen cooled MCT detector mounted directly on the reaction chamber. Spectral subtractions were performed using calibration spectra determined *in situ* or, where this was not possible, using scaled reference spectra taken from the literature. Optical ray-tracing and optical power density calculations were performed using the ZEMAX-XE Optical Design Program (15).

RESULTS AND DISCUSSION

FT-IR spectra of TEOS and ozone (Figure 1) were consistent with the literature (16,17). Figure 2 shows the *in situ* spectra of TEOS/O_3 under CVD process conditions at 50 and 300 °C. The spectra have been corrected for window deposits. At 50 °C the spectral features are readily assigned as a mixture of unreacted TEOS and ozone. The broad, weak absorption near 1750 cm^{-1} indicates some degree of reaction even at this temperature. The spectrum of the process gas at 300 °C exhibits strong features due to reaction products. Bands at ca. 2300 and 2140 cm^{-1} are due to CO_2, and CO, respectively. Multiple sharp absorptions between 1400 and 1600 cm^{-1} and above 3500 cm^{-1} are due to gas phase water. Absorptions at 1060, 1117 and 1085 cm^{-1} are common to all process gas analyses and can be assigned to overlapping bands from the precursors and silicon-containing reaction intermediates. The peaks at 1774 and 1795 cm^{-1} are due to oxidized organic fragments from the TEOS molecule. Kawahara et al. (18), assigned these bands to CH_3CHO and/or H_2CO. We have compared our process spectra with that of acetaldehyde published by the EPA (19) and found no matching absorptions, especially for ν_{C-H} vibrations. The process carbonyl absorptions are best assigned as due to the presence of a mixture of acetic acid (CH_3COOH) and formic acid (HCOOH). Spectra of acetic acid, determined within our apparatus show an excellent match with the process spectra. Mucha and Washington (20) made similar assignments for exhaust gas analyses of a TEOS/ozone reactor. The differences observed between our spectra and those of Kawahara are most likely due the different sampling methods. Our work and Mucha's deal with reacting flows under typical process conditions whereas Kawahara's spectra

were obtained on static mixtures of the reagents at relatively low temperatures (maximum 130 °C). Our *in situ* analysis of ozone at different reaction temperatures (14) suggests that, in Kawahara's work, the degree of ozone dissociation is significantly less than at normal process temperatures (300-400 °C). It has been shown that TEOS reacts only with atomic oxygen and not with molecular ozone (21). Therefore, Kawahara's results reflect a less strongly oxidizing ambient than this work or that of Mucha.

The presence of acetic acid in our reaction is consistent with mechanisms that have been proposed in the literature, i.e. that of Zachariah for the reaction of oxygen atoms with TEOS to generate acetaldehyde (5):

$$Si(C_2H_5O)_4 + O \rightarrow (C_2H_5O)_3SiOCHCH_3 + OH$$

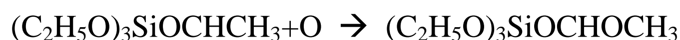

$$(C_2H_5O)_3SiOCHCH_3 + O \rightarrow (C_2H_5O)_3SiOCHOCH_3$$

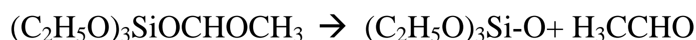

$$(C_2H_5O)_3SiOCHOCH_3 \rightarrow (C_2H_5O)_3Si\text{-}O + H_3CCHO$$

The acetaldehyde formed in these reactions may be further oxidized by atomic oxygen to acetic acid. Subsequent reactions of the organic fragments with atomic oxygen yield CO, CO_2 and water.

We are interested in using our approach to detect unstable intermediate species such as silanols and siloxane or siloxanol oligomers. The spectrum in Figure 2b shows that, while the starting materials and reaction products of the process are easily detected, spectral features due to intermediate species are not immediately apparent. An analysis of our experimental configuration suggests both a reason for this lack of information and a possible solution. The infrared beam of the spectrometer focuses at a point approximately 1 cm above the surface of the heated substrate. Modeling studies of TEOS/ozone reactions (22) show that the intermediate species are generated in a boundary layer that extends only millimeters from the substrate surface. We have performed similar studies using CHEMKIN-III (11,13) to assist in our data analysis and to predict the necessary system modifications that will optimize our system for the detection of reaction intermediates. We used kinetic mechanisms published by Gill and Ganguli (22) for our initial simulation, with the primary difference being our explicit assumption of the intermediate species as triethoxysilanol, $(C_2H_5O)_3SiOH$ and the use of non-linear temperature and gas velocity profiles (Figure 3). Using these values, we calculated k_1, the forward rate constant for the adsorption of intermediate, by means of the Moltz and Wise correction factor (12) with a sticking coefficient equal to 1 (as reported by Sorita et al [10]). The reverse rate constant k_{-1} was then obtained from the adsorption equilibrium constant K_{ads} that was reported by Gill and Ganguli and the relationship $K_{ads}=k_1/k_{-1}$. Both the forward and reverse rate constants for the adsorptions were thus explicit.

We have compared our simulation results with those of Gill and Ganguli (Figure 4). Our simulation predicted slightly higher concentrations of triethoxysilanol at the gas-solid interface and somewhat lower absolute peak concentration. The peak concentration

also occurs much closer to the surface in our simulation. As well, we find that the ozone concentration begins to decrease closer to the substrate surface than in Gill and Ganguli's model. The saturation effect of the TEOS flow rate on the deposition rate is well reproduced. Even though the asymptotic value is evidently the same in both cases (since we used the same surface reaction rate constant), the flow rates at which it is attained are greater in our case. Our simulation does not predict the same crossover characteristics for TEOS flow variations, as does that of Gill and Ganguli. We also predict the expected increase-decrease behavior of the deposition rate as either the total pressure or the wafer temperature is increased, but the maximum is reached at much higher pressures.

These differences can be understood in terms of the different velocity and temperature profiles employed in our work vs. that of Gill and Ganguli. The latter assumed linear gas velocity and temperature profiles between the showerhead and the wafer, whereas CHEMKIN-III predicts those profiles to be non-linear, as shown as in Figure 3. An independent evaluation of these profiles using FLUENT supports the CHEMKIN prediction. Using a non-linear temperature distribution, the consumption of reactants occurs further from the inlet in our model than in that of Gill and Ganguli. Under these conditions, intermediate concentrations in the gas phase are significantly lower when the flow impinges on the substrate surface. Therefore, the peak value for the intermediate concentration is weaker and nearer to the substrate surface in our model. We acknowledge that our reaction rate constants will have to be recalculated on the basis of a non-linear temperature distribution in order to be fully reliable. Both our and Gill and Ganguli's show that the peak concentrations of intermediate species are low and located close to the substrate surface and this has a profound effect on sampling considerations for real-time *in situ* analyses.

We have performed experiments to analyze this boundary layer using conventional spectrometer configurations by modifying our equipment to position the substrate inside of the spectrometer focal spot. A comparison of the spectra of processes performed at the same pressure but variable temperatures (Figure5) shows differences in the spectral features that may be related to the degree of oxidation of the system. This may be estimated by changes in the relative areas for the major peaks of CO_2, the final oxidation product of the reaction vs. CH_3COOH, an intermediate in the oxidation process. The peak areas associated with these species show reductions in the concentration of less oxidized product as the temperature of the reaction is increased. Absorptions in the region of the spectral region associated with Si-O-Si, Si-O-C and C-O are present, but strong overlap makes interpretation difficult. Figure 6 shows spectra of the oxide films produced by the reactions from Figure 5. Each spectrum shows an overlay of the spectra of the as-deposited film with that taken after aging in ambient air for seven days. The growth over time of infrared absorptions at ~960 and 3400 cm^{-1} indicate silanol and water incorporation in the film. It is apparent that for low temperature (300 °C) processes, higher pressures result in less hygroscopic films. The corresponding process spectra for these films show differences between 900-1200 cm^{-1}. It is tempting to develop detailed correlations of these differences with oxide properties. Unfortunately, the data is not of sufficient definition for quantitative evaluations in this area. The results discussed above

are promising in terms of their potential, but the optical configuration of the system needs to be further refined before accurate assignment of the spectral features can be made.

The use of a conventional FT-IR spectrometer in this application falls short in two critical areas. First, the focus size of the IR beam is too large to sample the thin boundary layer above the substrate. Second, the beam divergence is too great to permit effective use in the current designs for CVD reaction chambers. We have developed designs to reduce the focus size of ca. 12mm (conventional FT-IR) to ca. 2 mm. The design uses mid-IR fiber optics, both within the spectrometer and for I/O to the CVD chamber. This results in a reduced spot size at the focus since the fiber acts as a pseudo point source. We have also modified the collection of radiation at the source, to compensate for transmission losses in the fiber. We refined the source collection optics using the combination of a redesigned radiator, an optical cavity and fiber optics to increase the amount of infrared light launched into the fiber. These refinements permit a reduction in focal spot diameters to ca. 2-3 mm. We believe that refinement of the source shape and fabrication processes for the mirrors in our configuration can further enhance the launching efficiency and sample focus diameter.

We have used our experimental data for the modified source/collection optics as the basis for a complete simulation of a fiber based spectroscopic system suitable for sampling a CVD chamber. We used the commercially available Zemax-XE optical simulation package (15). Figure 7 shows a schematic of the simulated optical configuration. Tabulated data in the figure presents a comparison of the optical power calculated for each labeled point in the schematic. The optical power transferred to the interferometer from the modified source/collection optics (P_2) is seen to be 3X that calculated for a conventional configuration. The optical power transferred at the remaining points in the schematic do not retain this ratio between the modified and conventional designs, with the ratio increasing steadily greater at each transfer point. The reason for this lies in the fact that the modified design shows a small improvement in the divergence of the beam exiting the collection optics. Consequently, losses throughout the system are reduced and the power delivered to the detector is a factor of approximately 4.5 greater than that possible with conventional collection optics. The optical power at the detector may be compared to the value typical for an unmodified spectroscopic arrangement that does not use fiber transmission. For our unmodified spectrometer, this value is ca. 7mW. The introduction of fiber transmission into a conventional system reduces this power at the detector by almost a factor of 3, to 2.7 mW. Using the modified collection optics and fiber optic I/O, the power at the detector is actually increased over that of a conventional system that does not employ fiber I/O, with a value of approximately 12 mW. We are currently planning on implementing this modified spectrometer design in our experimental system.

The second critical factor for the successful application of FT-IR probes in CVD systems is the necessity to reduce the divergence as the beam transits the chamber. Without reduced divergence, significant occlusion of the beam will occur in systems processing 200 and 300 mm substrates. We are presently examining new design options in this area for reductions in divergence by conventional approaches such as changes in mirror size and by other, more novel routes.

CONCLUSION

FT-IR has been shown to be a useful, albeit not fully developed probe for CVD reactions in production-style systems. The method shows excellent sensitivity to reaction precursors and products. Conventional spectrometer configurations will have to be modified to effectively sample that region of the reactor space in which the reactive chemistry occurs. Our modeling studies and those of others have shown that this layer has a thickness of ca. 2-mm. If FT-IR spectroscopy is to be used to probe these reactions, the IR beam must sample this boundary layer. We have developed fiber optic approaches to spectrometer design and our simulations suggest that these approaches will at least partially fulfill the beam requirements for CVD reactor analyses.

ACKNOWLEDGEMENTS

We wish to acknowledge the financial support of the National Research Council of Canada under its IRAP program. We also wish to acknowledge support by the Canada-Israeli Research and Development Foundation.

REFERENCES

1. K. Fujino, Y. Nishimoto, N. Tokumasu and K. Maeda, J. Electrochem. Soc., **140**, 2922 (1993).
2. A. Kubo, T. Homma and Y. Murao, J. Electrochem. Soc., **143**, 1769 (1996).
3. T. Homma, M. Suzuki and Y. Murao, J. Electrochem. Soc., **140**, 3591 (1993).
4. I. A. Shareef, G. W. Rubloff and W. N. Gill, J. Vac. Sci. Technol., **B14**, 772 (1996).
5. O. Sanogo and M. R. Zachariah, J. Electrochem. Soc., **144**, 2919 (1997).
6. M. Adachi, K. Okuyama, N. Tohge, M. Shimada, J. Sato and M. Muroyama, Jpn. J. Appl. Phys., **33**, L447 (1994).
7. D. M. Dobkin, S. Mokhtari, M. Schmidt, A. Pant, L. Robinson and A. Sherman, J. Electrochem. Soc., **142**, 2332 (1995).
8. K. Okuyama, T. Fujimoto and T. Hayashi, Ceramics Processing, **43**, 2688 (1997).
9. T. Satake, T. Sorita, H. Fujioka, H. Adachi and H. Nakajima, Jpn. J. Appl. Phys., **33**, 3339 (1994).
10. T. Sorita, S. Shiga, K. Ikuta, Y. Egashiba and H. Komiyama, J. Electrochem. Soc., **140**, 2952 (1993).
11. Commercial Software from Reaction Design, San Diego, CA.
12. M. E. Coltrin, R. J. Kee, F. M. Rupley, E. Meeks, "Surface Chemkin-III", Sandia National Laboratories, SAN96-8217 (1996).
13. Thomas K. Whidden, Sarah Doiron and Sun Young Lee, *Proceedings of The First International Symposium on Dielectric Materials for Advanced Packaging*, San Diego, CA, editors - W. D. Brown, S. S. Ang, M. Loboda, B. Sammakia, R. Singh and H. S. Rathore, **PV 98-3**, p. 326, The Electrochemical Society, Pennington, NJ, May 3-8, (1998).
14. Thomas K. Whidden and Sarah Doiron, *Proceedings of the 1998 International Conference on Characterization and Metrology for ULSI Technology*, Gaithersburg, MD, March 23-27, 1998, *in press*.
15. Commercial Software from Focus Software, Inc. P.O. Box 18228, Tucson, Arizona 85731 USA.

16. J. A. O'Neill, M. L. Passow and T. J. Cotler, J. Vac. Sci. Technol., **A12**, 839 (1994).
17. M. G. M. van der Vis, R. J. M. Konings, A. Oskam and T. L. Snoeck, J. Mol. Struct., **274**, 47 (1992).
18. T. Kawahara, A. Yuuki and Y. Matsui, Jpn. J. Appl. Phys., **31**, 2925 (1992).
19. Spectral database of David Sullivan - Univ. of Texas/Chem. Eng. Dept., Web URL: http://www.galactic.com/Datalib/slvnftir/slvnftir.htm/
20. J. A. Mucha and J. Washington, Mat. Res. Soc. Proc., **334**, 31 (1994).
21. M. Matsuura, Y. Hayashide, H. Kotani and H. Abe, Jpn. J. Appl. Phys., **30**, 1530 (1991).
22. W. N. Gill and S. Ganguli, J. Vac. Sci. Technol., **B15**, 948 (1997).

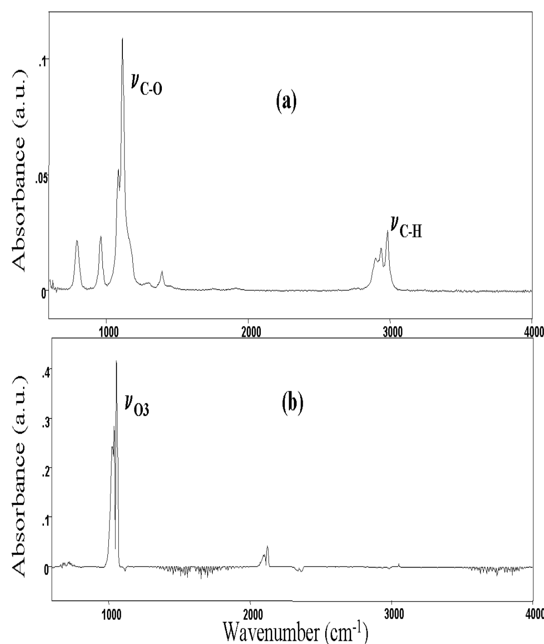

Figure 1. The *in situ* FT-IR spectra of (a) TEOS and (b) ozone. The TEOS spectum was obtained *in situ* under typical process conditions (T=300 °C, P=500 Torr, N_2 diluent flow = 3 slm). The ozone spectrum was taken under similar conditions, except that T=22 °C to avoid excessive dissociation.

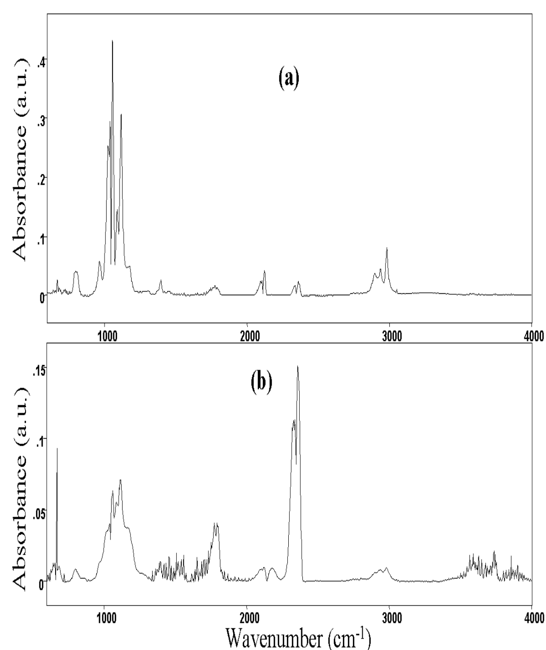

Figure 2. The *in situ* spectrum of TEOS/ozone mixtures determined within the CVD reactor. Total pressure = 500 Torr, N_2 diluent flow = 3 slm, O_3 = 8%, Total O_2 flow = 2 slm. (a) Spectrum obtained with the substrate temperature at 50 °C. (b) Spectrum obtained with the substrate temperature set at 300 °C.

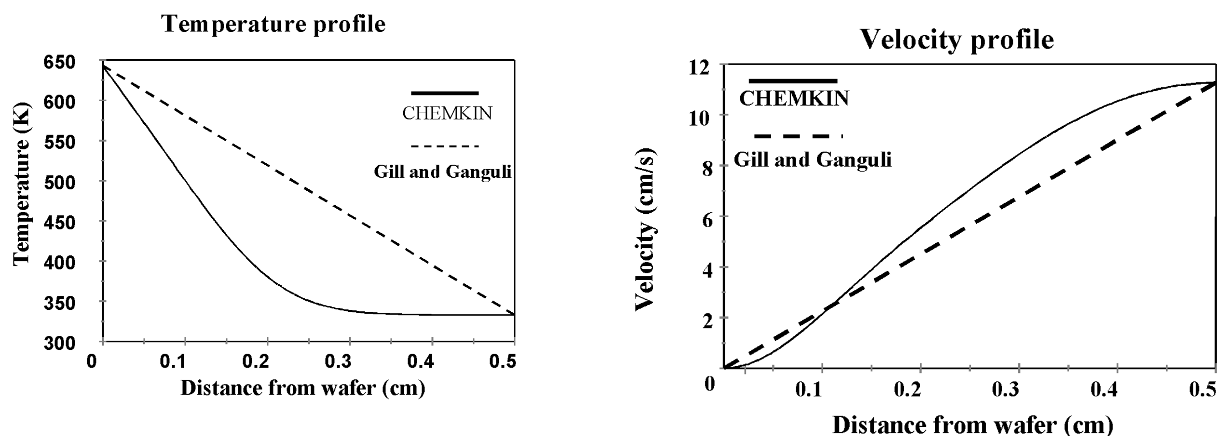

Figure 3. The temperature and gas velocity profiles used in this simulation, as compared with those employed by Gill and Ganguli. Lines denoted as "Spin" were generated by the routine within CHEMKIN-III used to calculate temperature and gas velocity profiles.

Proceedings of the Symposium on Fundamental Gas-Phase and
Surface Chemistry of Vapor-Phase Materials Synthesis,
PV98-28, p. 153,The Electrochemical Society, 1998.

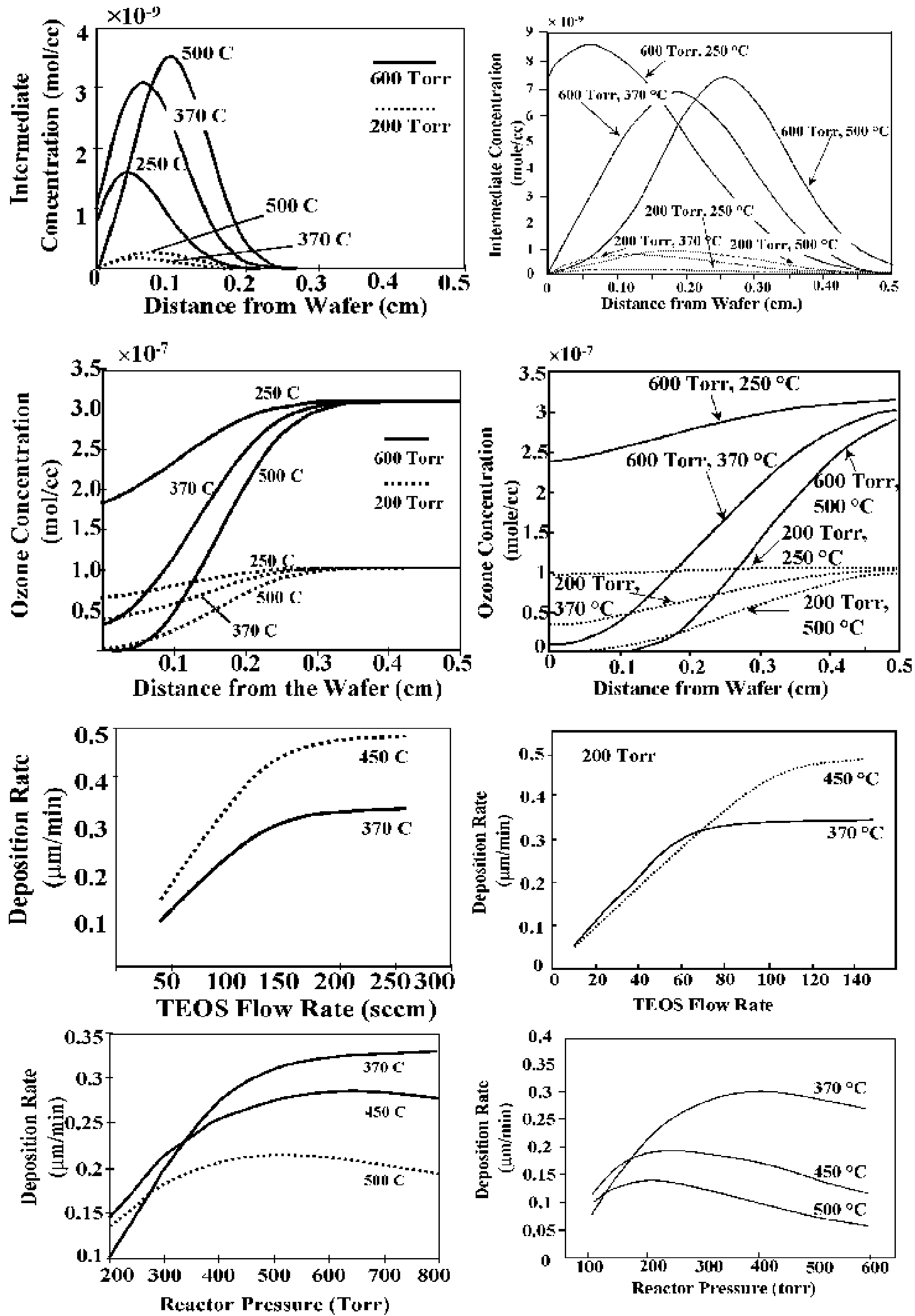

Figure 4. CHEMKIN-III simulation results for TEOS/ozone CVD in our reactor configuration. Our results (Left column) are compared with those reported by Gill and Ganguli (ref. 12, Right column). Showerhead temperature was set at 60°C and the inlet flow rates were: N_2=20,000 sccm, O_2=10,000 sccm, O_3=325 sccm, TEOS=41 sccm.

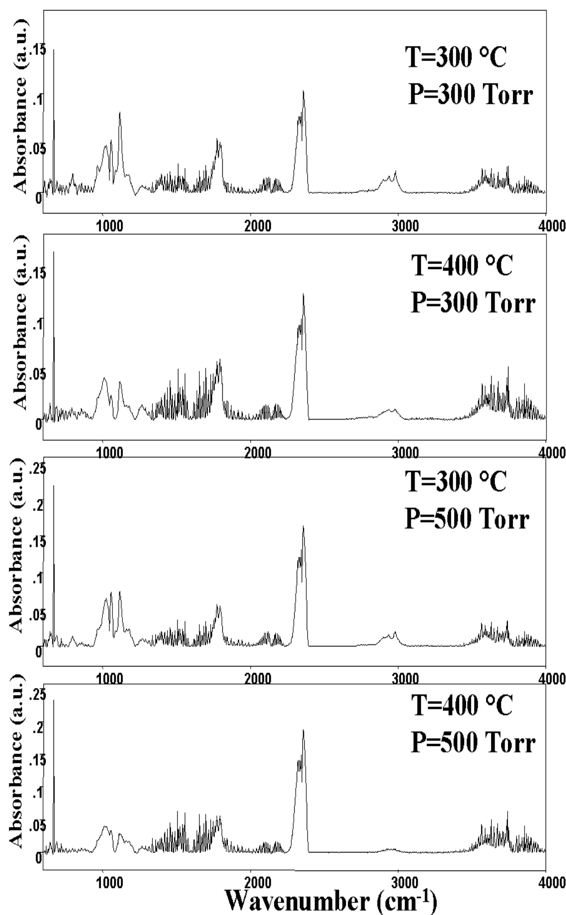

Figure 5. Process gas spectra obtained with the substrate immersed in the infrared beam (O_3=8%, O_2=2 slm, TEOS N_2 = 600 sccm).

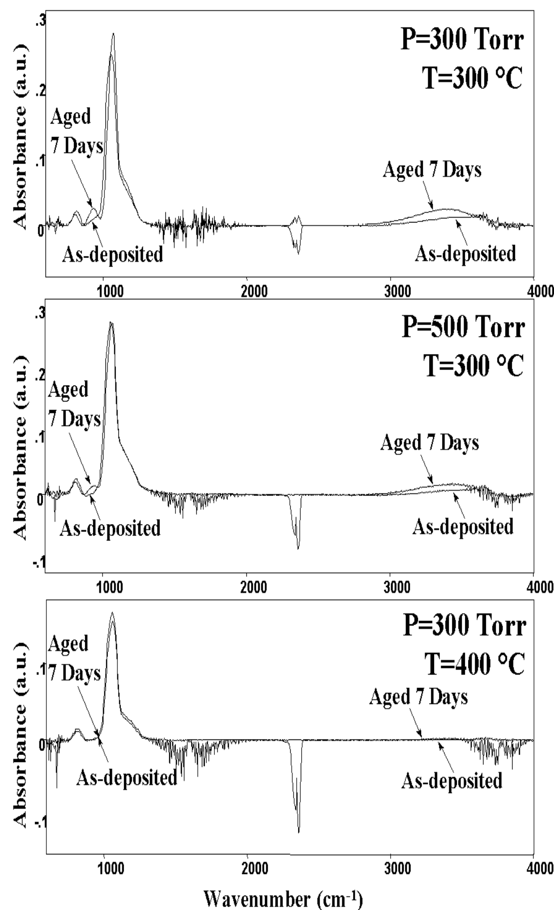

Figure 6. Infrared spectra of the silicon dioxide thin films obtained as products of the reactions shown in Figure 5.

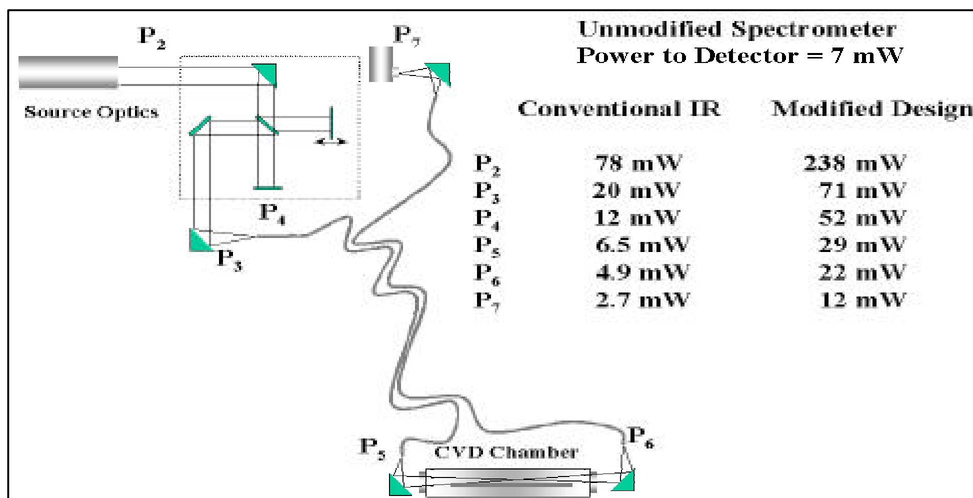

	Conventional IR	Modified Design
P_2	78 mW	238 mW
P_3	20 mW	71 mW
P_4	12 mW	52 mW
P_5	6.5 mW	29 mW
P_6	4.9 mW	22 mW
P_7	2.7 mW	12 mW

Figure 7. Simulated optical configuration for a fiber optics based spectrometer. Tabulated values are for a conventional and modified designs with fiber I/O.